Investigation upon the performance of piezoelectric energy harvester with flexible extensions

Maoying Zhou, Weiting Liu, Yang Fu

1. Model Description

We seek to investigate the influence of a flexible extension upon the overall performance of a classic piezoelectric cantilever beam energy harvester. In our problem, the energy harvester is comprised of two parts: the primary beam part and the beam extension part, as shown in Figure 1.

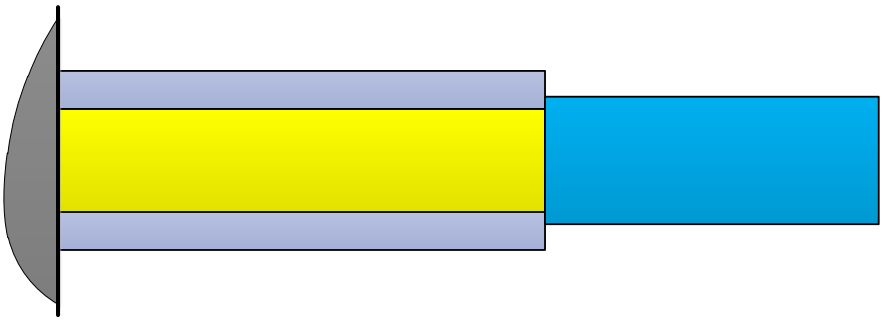

Figure 1: Schematic configuration of the piezoelectric energy harvester with flexible extension.

Following the classical analyzing process of piezoelectric bimorph cantilever beams [1, 2], we can simply list the following dimensional equations for the piezoelectric primary beam part as:

$$\begin{cases} M_p(x_1,t) = B_p \dfrac{\partial^2 w_1(x_1,t)}{\partial x_1^2} - e_p V_p(t) \\ q_p(x_1,t) = e_p \dfrac{\partial^2 w_1(x_1,t)}{\partial x_1^2} + \epsilon_p V_p(t), \end{cases} \tag{1}$$

where where $M_p(x_1,t)$ is the moment at cross section of x_1 and $q_p(x_1,t)$ is the corresponding line charge density on the electrode. $w_1(x_1,t)$ is the displacement function of the primary beam part with $0 \le x_1 \le l_p$ and $V_p(t)$ is the voltage across the electrodes. The corresponding coefficients B_p, e_p, and ϵ_p are defined as

$$B_p = \frac{2}{3} b \left\{ E_s h_s^3 + c_{11}^E \left[(h_s + h_p)^3 - h_s^3 \right] \right\}, \quad e_p = b e_{31} \left(h_s + \frac{1}{2} h_p \right), \quad \epsilon_p = \frac{b \epsilon_{33}^S}{2 h_p} \tag{2}$$

in which c_{11}^E and E_s are the elastic constants of the piezoelectric layer and the structure layer, respectively, e_{31} is the piezoelectric charge constant of the piezoelectic layer, ϵ_{33}^S is the dielectric constant of the piezoelectric layer, h_s and h_p are the half structure layer thickness and piezoelectric layer thickness, respectively, l_p is the length of the primary beam part, and b is the width of the primary beam part.

In terms of the mechanical balance, the equation of a piezoelectric beam can be established using the Euler-Bernoulli assumptions as follows

$$B_p \frac{\partial^4 w_1(x_1,t)}{\partial x_1^4} + m_p \frac{\partial^2 w_1(x_1,t)}{\partial t^2} = 0 \tag{3}$$

where $m_p = 2b(\rho_s h_s + \rho_p h_p)$ is the line mass density of the primary beam part with ρ_s and ρ_p being the volumetric density of the structure layer and the piezoelectric layer, respectively. In turn,

principally the piezoelectric energy harvester can be regarded as a current source. So we need to know the charge accumulated on the electrode $Q_p(t)$, which is calculated as

$$Q_p(t) = \int_0^{l_p} q_p(t)\ dx_1 \ = \ e_p \left[\frac{\partial w_1(x_1,t)}{\partial x_1}\right]\Big|_0^{l_p} + C_p V_p(t) \tag{4}$$

where $C_p = \epsilon_p l_p$ is the inherent capacitance of the piezoelectric layer. According to the Kirchhoff's law, the electric equilibrium equation is

$$\frac{dQ_p(t)}{dt} + \frac{V_p(t)}{R_l} = 0 \tag{5}$$

where R_l is the externally connected resistive load.

When it comes to the beam extension part ($0 \le x_2 \le l_e$), the governing equations are

$$B_e \frac{\partial^4 w_2(x_2,t)}{\partial x_2^4} + m_e \frac{\partial^2 w_2(x_2,t)}{\partial t^2} = 0 \tag{6}$$

where $w_2(x_2,t)$ is the displacement of the extension beam at position $0 \le x_2 \le l_e$, $B_e = \frac{2}{3} b h_e^3$ is the equivalent bending stiffness of the extension beam, $m_e = \rho_e h_e$ is the line mass density of the extension beam, ρ_e is the volumetric mass density of the extension beam, h_e is the half thickness of the extension beam, and l_e is the length of the extension beam. As a result, the defining relations for the cross section moment $M_e(x_2,t)$ at the position x_2 is

$$M_e(x_2,t) = B_e \frac{\partial^2 w_2(x_2,t)}{\partial x_2^2}. \tag{7}$$

The related boundary conditions are listed as follows. When $x_1 = 0$ at the fixed end of the primary beam,

$$w_1(0,t) = w_b(t), \quad w_1'(0,t) = 0, \tag{8}$$

where $w_b(t)$ is the base excitation displacement function. Usually we use a harmonic vibration in the experiment where $w_b(t) = Re\left\{\xi_b e^{j\sigma t}\right\}$ with σ being the angular frequency of the base excitation signal and $j = \sqrt{-1}$ being the imaginary unit. To be more accurate, the amplitude ξ_b is generally set to be a real constant designated by the controller. At the connection point of the primary beam and the beam extension where $x_1 = l_p$ and $x_2 = 0$,

$$\begin{cases} w_1(l_p,t) = w_2(0,t) \\ \dfrac{\partial w_1(l_p,t)}{\partial x_1} = \dfrac{\partial w_2(0,t)}{\partial x_2} \\ B_p \dfrac{\partial^2 w_1(l_p,t)}{\partial x_1^2} - e_p V_p(t) = B_e \dfrac{\partial^2 w_2(0,t)}{\partial x_2^2} \\ B_p \dfrac{\partial^3 w_1(l_p,t)}{\partial x_1^3} = B_e \dfrac{\partial^3 w_2(0,t)}{\partial x_2^3} \end{cases}, \tag{9}$$

and at the free end of the beam extension where $x_2 = l_e$, we have

$$\frac{\partial^2 w_2(l_e,t)}{\partial x_2^2} = 0, \quad \frac{\partial^3 w_2(l_e,t)}{\partial x_2^3} = 0 \tag{10}$$

1.1. Harmonic Balance Analysis

Generally in the literature [1, 2], mode decomposition method or finite element method are used to solve the above described equations. Here in this contribution, as we are interested in the steady state response of the piezoelectric energy harvester, and the above described system are linear, harmonic balance method is used. Hence, as a result of the base excitation $w_b(t) = Re\left\{\xi_b e^{j\sigma t}\right\}$, we can set the steady state response of the displacements $w_1(x_1,t)$ and $w_2(x_2,t)$ of the primary beam and the beam extension respectively as

$$w_1(x_1,t) = \tilde{w}_1(x_1)e^{j\sigma t}, \quad w_2(x_2,t) = \tilde{w}_2(x_2)e^{j\sigma t}, \tag{11}$$

the steady state voltage response $V_p(t)$ and charge accumulation $Q_p(t)$ as

$$V_p(t) = \tilde{V}_p e^{j\sigma t}, \quad Q_p(t) = \tilde{Q}_p e^{j\sigma t}, \tag{12}$$

and the cross section moment $M_p(x_1, t)$ and $M_e(x_2, t)$ described as

$$M_p(x_1, t) = \tilde{M}_p(x_1) e^{j\sigma t}, \quad M_e(x_2, t) = \tilde{M}_e(x_2) e^{j\sigma t}. \tag{13}$$

As a result, the system of equations for the piezoelectric energy harvester can be summarized as

$$\begin{cases} B_p \dfrac{\partial^4 \tilde{w}_1(x_1)}{\partial x_1^4} - m_p \sigma^2 \tilde{w}_1(x_1) = 0 \\ B_e \dfrac{\partial^4 \tilde{w}_2(x_2)}{\partial x_2^4} - m_e \sigma^2 \tilde{w}_2(x_2) = 0 \\ j\sigma \tilde{Q}_p + \dfrac{\tilde{V}_p}{R_l} = 0 \end{cases}, \tag{14}$$

$$\begin{cases} \tilde{M}_p(x_1) = B_p \dfrac{\partial^2 \tilde{w}_1(x_1)}{\partial x_1^2} - e_p \tilde{V}_p \\ \tilde{Q}_p = e_p \left[\dfrac{\partial \tilde{w}_1(x_1)}{\partial x_1} \right] \Big|_0^{l_p} + C_p \tilde{V}_p \\ \tilde{M}_e(x_2) = B_e \dfrac{\partial^2 \tilde{w}_2(x_2)}{\partial x_2^2} \end{cases}, \tag{15}$$

and the boundary conditions become

$$\begin{cases} \tilde{w}_1(0) = \xi_b, & \dfrac{\partial \tilde{w}_1}{\partial x_1}(0) = 0 \\ w_1(l_p, t) = w_2(0, t), & \dfrac{\partial \tilde{w}_1(l_p)}{\partial x_1} = \dfrac{\partial \tilde{w}_2(0)}{\partial x_2} \\ B_p \dfrac{\partial^2 \tilde{w}_1(l_p)}{\partial x_1^2} - e_p \tilde{V}_p = B_e \dfrac{\partial^2 \tilde{w}_2(0)}{\partial x_2^2}, & B_p \dfrac{\partial^3 \tilde{w}_1(l_p)}{\partial x_1^3} = B_e \dfrac{\partial^3 \tilde{w}_2(0)}{\partial x_2^3} \\ \dfrac{\partial^2 \tilde{w}_2(l_e)}{\partial x_2^2} = 0, & \dfrac{\partial^3 \tilde{w}_2(l_e)}{\partial x_2^3} = 0 \end{cases}. \tag{16}$$

From the equations (14), (15), and (16), we can eliminate the electrical quantities $\tilde{Q}_p$ and $\tilde{V}_p$ by incorporating them into the boundary conditions. Actually, from equations (14) and (15), we have

$$\tilde{V}_p = \frac{j\sigma R_l e_p}{j\sigma R_l C_p + 1} \left[\frac{\partial \tilde{w}_1(x_1)}{\partial x_1} \right] \Big|_0^{l_p} \tag{17}$$

which can actually be used to eliminate the term $\tilde{V}_p$ in the boundary conditions (16). In the end, we can simplify the problem as a combination of the governing equations

$$\begin{cases} B_p \dfrac{\partial^4 \tilde{w}_1(x_1)}{\partial x_1^4} - m_p \sigma^2 \tilde{w}_1(x_1) = 0 \\ B_e \dfrac{\partial^4 \tilde{w}_2(x_2)}{\partial x_2^4} - m_e \sigma^2 \tilde{w}_2(x_2) = 0 \end{cases} \tag{18}$$

and the boundary conditions

$$\begin{cases} \tilde{w}_1(0) = \xi_b, & \dfrac{\partial \tilde{w}_1}{\partial x_1}(0) = 0 \\ \tilde{w}_1(l_p) = \tilde{w}_2(0), & \dfrac{\partial \tilde{w}_1(l_p)}{\partial x_1} = \dfrac{\partial \tilde{w}_2(0)}{\partial x_2} \\ B_p \dfrac{\partial^2 \tilde{w}_1(l_p)}{\partial x_1^2} + \dfrac{j\sigma R_l e_p^2}{j\sigma R_l C_p + 1} \dfrac{\partial \tilde{w}_1(l_p)}{\partial x_1} = B_e \dfrac{\partial^2 \tilde{w}_2(0)}{\partial x_2^2}, & B_p \dfrac{\partial^3 \tilde{w}_1(l_p)}{\partial x_1^3} = B_e \dfrac{\partial^3 \tilde{w}_2(0)}{\partial x_2^3} \\ \dfrac{\partial^2 \tilde{w}_2(l_e)}{\partial x_2^2} = 0, & \dfrac{\partial^3 \tilde{w}_2(l_e)}{\partial x_2^3} = 0 \end{cases}. \tag{19}$$

which actually manifests as a boundary value problem.

2. Dimensionless Problem

Using the following dimensionless group

$$\tilde{w}_1, \tilde{w}_2 \sim \xi_b, \quad \tilde{x}_1 \sim l_p, \quad \tilde{x}_2 \sim l_e \tag{20}$$

we can nondimensionalize the above formulated boundary value problem with respect to the following variables:

$$\tilde{w}_1 = \xi_b u_1, \quad \tilde{w}_2 = \xi_b u_2, \quad \tilde{x}_1 = l_p x, \quad \tilde{x}_2 = l_e x. \tag{21}$$

Note that here we use one independent space variable x to nondimensionalize two previously used variables x_1 and x_2. This comes from the fact that the variables x_1 and x_2 are not coupled with each other in the sense that the primary beam and the extension beam do not overlap each other except for their joint point where $x_1 = l_p$ and $x_2 = 0$. Thus the two variables do not occur in the equations simultaneously except for the boundary conditions. As for the boundary conditions, the change of variables does not affect the values of the equations. Therefore, the two parts of the piezoelectric energy harvester beam are in fact independent of each other except for the joining point. In one word, the equation (21) does not change the problem in essence.

Hence, the above boundary value problem is further changed into the combination of the governing equations

$$\begin{cases} \dfrac{B_p}{l_p^4} u_1'''' - m_p \sigma^2 u_1 = 0 \\ \dfrac{B_e}{l_e^4} u_2'''' - m_e \sigma^2 u_2 = 0 \end{cases} \tag{22}$$

and the boundary conditions

$$\begin{cases} u_1(0) = 1, \quad u_1'(0) = 0 \\ u_1(1) = u_2(0), \quad \dfrac{1}{l_p} u_1'(1) = \dfrac{1}{l_e} u_2'(0) \\ \dfrac{B_p}{l_p^2} u_1''(1) + \dfrac{j\sigma R_l e_p^2}{j\sigma R_l C_p + 1} \dfrac{1}{l_p} u_1'(1) = \dfrac{B_e}{l_e^2} u_2''(0), \quad \dfrac{B_p}{l_p^3} u_1'''(1) = \dfrac{B_e}{l_e^3} u_2'''(0) \\ u_2''(1) = 0, \quad u_2'''(1) = 0 \end{cases}. \tag{23}$$

in which the prime means the derivative with respect to x. The equations can again be organized in a more compact form

$$\begin{cases} u_1'''' - \nu^2 u_1 = 0 \\ u_2'''' - \nu^2 \lambda_m \lambda_l^4 / \lambda_B u_2 = 0 \end{cases} \tag{24}$$

and the boundary conditions

$$\begin{cases} u_1(0) = 1, \quad u_1'(0) = 0 \\ u_1(1) = u_2(0), \quad \lambda_l u_1'(1) = u_2'(0) \\ u_1''(1) + \dfrac{j\nu\beta}{j\nu\beta + 1} \alpha^2 u_1'(1) = \lambda_B / \lambda_l^2 u_2''(0), \quad u_1'''(1) = \lambda_B / \lambda_l^3 u_2'''(0) \\ u_2''(1) = 0, \quad u_2'''(1) = 0 \end{cases}. \tag{25}$$

where

$$\nu = \sigma \sqrt{\frac{m_p l_p^4}{B_p}}, \quad \lambda_B = \frac{B_e}{B_p}, \quad \lambda_m = \frac{m_e}{m_p}, \quad \lambda_l = \frac{l_e}{l_p} \tag{26}$$

$$\beta = R_l C_p \sqrt{\frac{B_p}{m_p l_p^4}}, \quad \alpha = e_p \sqrt{\frac{l_p}{C_p B_p}} \tag{27}$$

The system (24) and (25) is a two-point boundary value problem. The problem can readily be solved by a Chebyschev collocation method using the MATLAB package *Chebfun* [3].

Table 1: Geometric, material, and electromechanical parameters of the simulation for piezoelectric energy harvester with flexible extension

Parameter item	**Parameter value**
Length of the primary beam, l_p (mm)	100
Width of the whole energy harvester, b (mm)	20
Half thickness of the structure, h_s (mm)	0.25
Thickness of the piezoelectric layer, h_p (mm)	0.2
Young's modulus of the structure, Y_s (Gpa)	100
Young's modulus of the piezoelectric layer, Y_p (Gpa)	66
Mass density of the substructure, ρ_s (kg/m^3)	7165
Mass density of the piezoelectric layer, ρ_p (kg/m^3)	7800
piezoelectric constant, d_{31} (pm/V)	-190
Permittivity, ϵ_{33}^S (nF/m)	15.93
Length of the beam extension, l_e (mm)	30
Young's modulus of the beam extension, Y_e (Gpa)	2.3
Mass density of the beam extension, ρ_e (kg/m^3)	1.38
Half thickness of the structure, h_e (mm)	0.25

3. Influence of extension part upon energy harvester performance

The basic geometry and material properties of the materials used in the proposed piezoelectric energy harvester with flexible extensions are summarized in Table 1. Note that some of the parameters, like length l_e, Young's modulus Y_e, and volumetric density ρ_e of the beam extension, are actually changing across different simulations. In the simulation, base excitation frequency fr and external load resistance R_l, which change the dimensionless values of ν and β, respectively, are of critical importance in the sense that these two parameters reflect the influence of vibration source frequency spectrum and external load circuit. For every set of parameter values, we set the base excitation frequency fr to change from 1 Hz to 100 Hz, which covers the usual frequency range of natural vibration sources, and set the load resistance R_l to change from 1 Ω to 10 $M\Omega$, which is inspired by the Ref. [1] and takes into account the dielectric property of piezoelectric materials. Actually, when the load resistance $R_l = 1\ \Omega$, the piezoelectric energy harvester is said to be in a short-circuit condition as the general equivalent resistance of the structure is much larger than R_l. On the other hand, when $R_l = 10\ M\Omega$, the system is close to an open-circuit condition where no external load is connected to the output electrodes.

In the following, we will investigate the influences of length l_e, Young's modulus Y_e, and volumetric density ρ_e of the beam extension upon the performance of the piezoelectric energy harvester with flexible extensions separately.

3.1. Beam extension length l_e or length ratio λ_l

The presence of the beam extension is primarily indicated by the beam extension length l_e, or equivalently the length ratio λ_l. When $\lambda_l = 0.0$, no beam extension is attached to the primary beam and the resultant piezoelectric energy harvester reduces to the classic piezoelectric energy harvesting bimorph [1], which is referred to as a reference for comparison. In this contribution, the range of length ratio λ_l to be considered is set to be $0.0 \leq \lambda_l \leq 1.0$. For each value of length ratio λ_l, the base excitation problem is solved with respect to different base excitation frequency fr and load resistance R_l. In this process, the Young's modulus of the beam extension part is set to be $Y_e = 2.3\ GPa$ while its volumetric density is set to be $\rho_e = 1.38 \times 10^3\ kg/m^3$.

In the first place, we would like to explore the influence of base excitation frequency fr upon performance of the piezoelectric energy harvester at different values of load resistance R_l and length ratio λ_l. Let the frequency range of interest be $1 - 100\ Hz$. The length ratio λ_l is chosen to be 0.0, 0.2, 0.4, 0.6, 0.8, or 1.0, and load resistance R_l is chosen to be $10^0\ \Omega$, $10^2\ \Omega$, $10^4\ \Omega$, or $10^6\ \Omega$. The resulting amplitudes of output voltage V_p and output power P_p are plotted against base excitation frequency fr in Figure 2 and Figure 3, respectively. In this process, the values of beam extension part density ρ_e and Young's modulus Y_e are kept unchanged, so do the values of λ_m and λ_B.

According to Figure 2 and Figure 3, for the given values λ_B and λ_m, frequency response of the piezoelectric energy harvester in the interested frequency range changes in accordance with the extension length l_e and thus the length ratio λ_l.

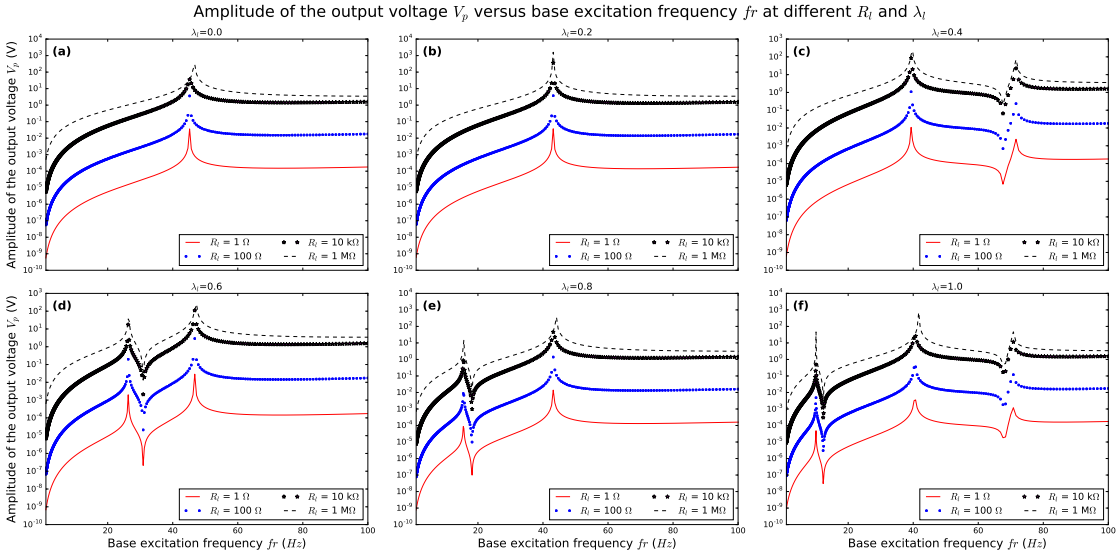

Figure 2: Output voltage V_p (amplitude) of the piezoelectric energy harvester with flexible extension versus base excitation frequency fr at different length ratio λ_l and load resistance R_l.

When λ_l is relatively small, say $\lambda_l = 0.2$, as shown in Figure 2(b), frequency response of the $PEHFE$ piezoelectric energy harvester with flexible extension is almost the same as that of the $CPEH$ case where $\lambda_l = 0.0$. That is to say, there is only resonant peak in the considered frequency range and the corresponding resonant frequency is around 42 Hz for different values of load resistance R_l. Therefore we can conclude that in this situation, the beam extension part is playing a negligible role in the motion of the primary beam part. As a result, energy harvesting performances of the proposed piezoelectric energy harvesters with flexible extensions are similar to that of a classic piezoelectric energy harvester.

With the increase of the length ratio λ_l, say $\lambda_l = 0.4$, 0.6, or 0.8, as shown in Figure 2(b), (c), and (d), respectively, there begins to exist an extra resonant and anti-resonant mode in the considered frequency range, compared with that of the case of no flexible extension where $\lambda_l = 0.0$. An increase of the value of λ_l causes the decrease of the resonant and anti-resonant frequencies of the newly occurring mode. What's more, for the cases of $\lambda_l = 0.4$ and 0.6, the resonant frequency of the previously existing mode, which corresponds to the first resonant mode of a classic piezoelectric energy harvester, is shifted by an obvious degree. This can be explained as follows. The motion of the proposed piezoelectric energy harvester with flexible extension is controlled by the primary beam part and the beam extension part. With the increase of λ_l, resonant frequency of the beam extension part approaches that of the primary beam. Thus the two parts interact with each other at a high level. resonant frequency of the whole piezoelectric energy harvester with flexible extension is therefore tuned by the beam extension part. When the resonant frequency of the beam extension is far small than that of the primary beam, which is the case for $\lambda = 0.8$, as shown in Figure 2(d), the two parts have little effect upon each other.

If we further increase the length ratio to $\lambda_l = 1.0$, more resonant and anti-resonant modes occur in the considered frequency range. It can be found from Figure 2(d) and Figure 3(d) that, amplitude of the output voltage V_p and output power P_p at the newly occurring resonant mode is comparable in order of magnitude to that of the classic piezoelectric energy harvester.

In this view, attachment of the flexible extension part actually increases the working frequency range of the piezoelectric energy harvester, as typical piezoelectric energy harvesters rely on resonant modes to work. On the other hand, the flexible extension also provides a way to tune the bandwidth of a piezoelectric energy harvester. An obvious way to do so is to choose the parameters of the beam extension part, so that the beam extension part and the primary beam part have similar resonant frequency and interact strongly with each other. The point to be noticed is the existence of anti-resonant modes. They correspond to low output voltage and output power, and to some degree narrows the bandwidth of the energy harvester. However, it is still not worse than an otherwise non-resonant vibration, as in both cases the electrical output of the piezoelectric energy harvester is unusable.

In the second place, we investigate the influence of load resistance R_l upon performance of the

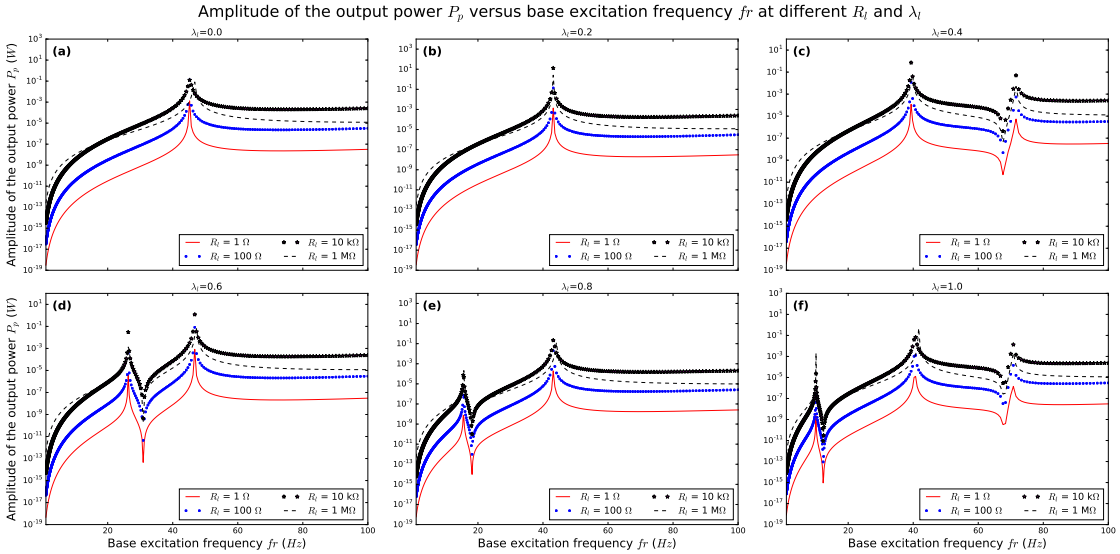

Figure 3: Output power P_p (amplitude) of the piezoelectric energy harvester with flexible extension versus base excitation frequency fr at different length ratio λ_l and load resistance R_l.

piezoelectric energy harvester at different values of base excitation frequency fr and length ratio λ_l. The resulting amplitudes of output voltage V_p and output power P_p are shown in Figure 4 and Figure 5, respectively. It is obvious that in the range of low R_l, a power law exists between the amplitudes of output voltage V_p and output power P_p and load resistance R_l. For all the chosen values of base excitation frequency fr, the increase of R_l leads to an increase in V_p. Ultimately, V_p approaches asymptotically to a limit value V_p^{lim}. This value actually corresponds to the amplitude of open-circuit output voltage of the piezoelectric energy harvester. At the same time, the value of P_p exhibits an obvious maximum at some values of R_l between 10 $k\Omega$ and 1 $M\Omega$. And on both sides away from the maximum value, we see also a power law between the value of R_l and P_p, as shown in Figure 5. This indicates that an asymptotic analysis may help us to simplify the analysis of performance of piezoelectric energy harvesters. But this is out of the scope of our current contribution and will be covered in the future research.

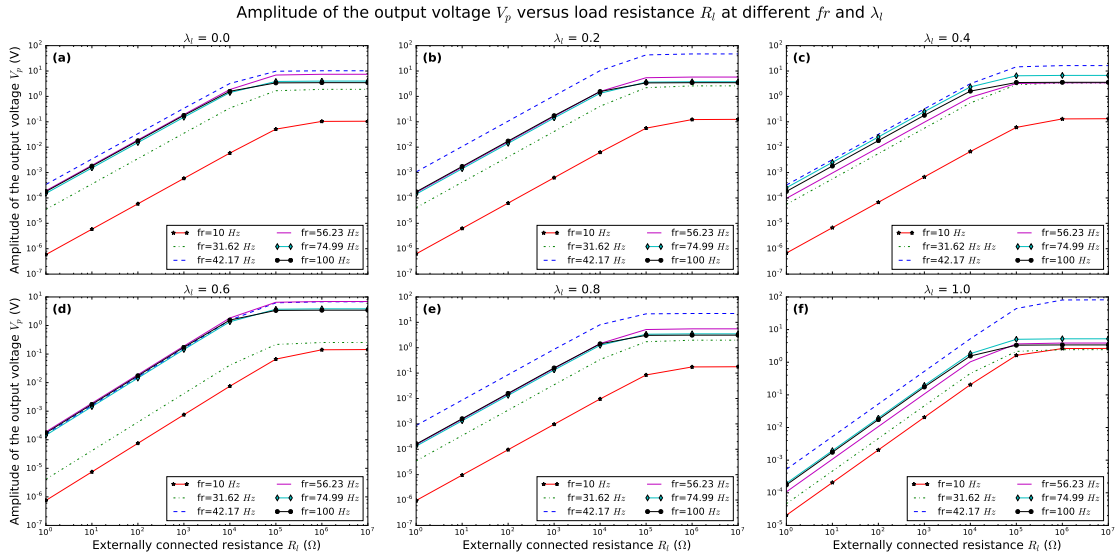

Figure 4: Output voltage V_p (amplitude) of the piezoelectric energy harvester with flexible extension versus load resistance R_l at different frequency fr and length ratio λ_l.

In the third place, at different values of fr and R_l, we directly plot the amplitudes of V_p and P_p with respect to λ_l, which are shown in Figure 6 and Figure 6, respectively. It is shown that at given values of R_l and fr, output performances of the proposed piezoelectric energy harvesters can

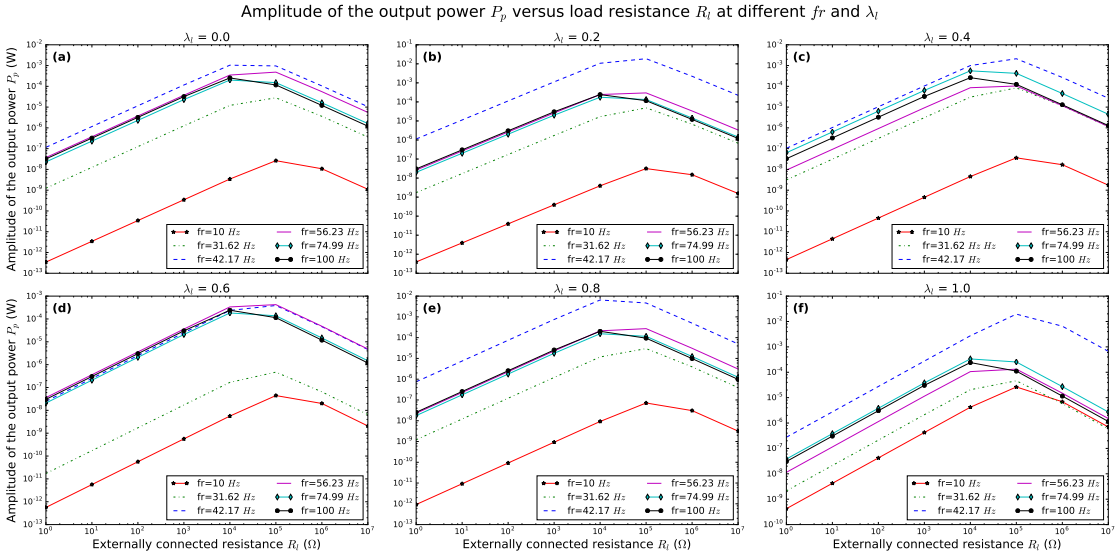

Figure 5: Output power P_p (amplitude) of the piezoelectric energy harvester with flexible extension versus load resistance R_l at different frequency fr and length ratio λ_l.

be tuned by the parameter λ_l. For example, when $fr = 31.62\ Hz$ and $R_l = 10\ k\Omega$, a maximum peak of V_p and P_p is found around $\lambda_l = 0.5$. Compared with the case of no flexible extension ($\lambda_l = 0$), the amplitude of output voltage V_p is about 13 times larger, while the amplitude of output power P_p is about 3 times larger. Similar phenomena can be found when $fr = 42.17\ Hz$. This indicates that the addition of the flexible extension can substantially increase the output performance of a piezoelectric energy harvester. It should be noted that in case of large values of fr, like $fr = 100\ Hz$, the tuning performance of the flexible extension is no longer significant.

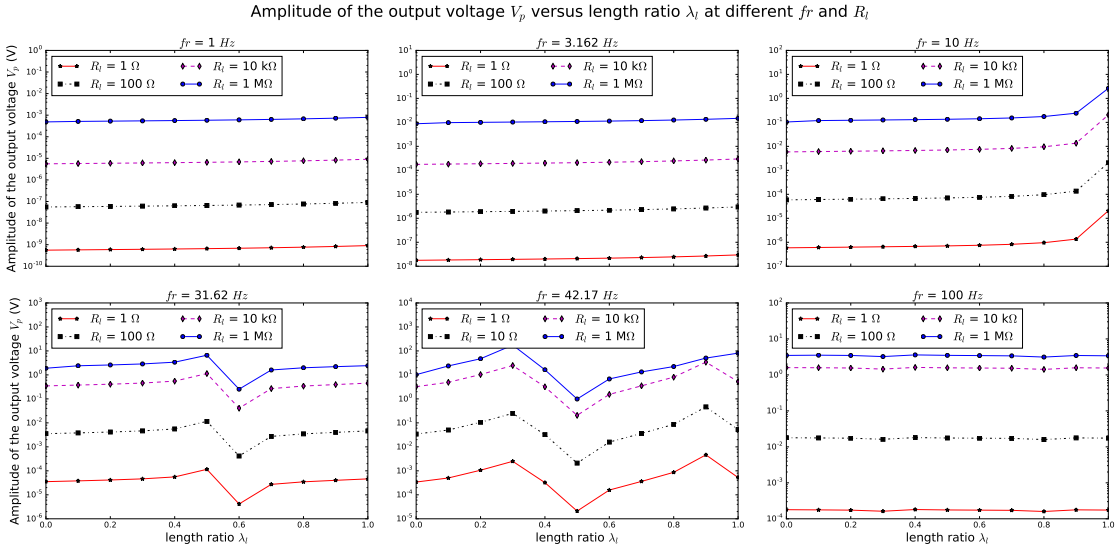

Figure 6: Output voltage V_p (amplitude) and output power P_p (amplitude) of the piezoelectric energy harvester with flexible extension versus length ratio λ_l at different frequency f and load resistance R_l. to be revised in the legend, add label (a), (b)

3.2. Beam extension Young's modulus Y_e or bending stiffness ratio λ_B

To investigate the influence of bending stiffness ratio λ_B upon the performance of the piezoelectric energy harvester with flexible extension, we set different values of Young's modulus Y_e of the beam extension part to change the values of λ_B. Considering the properties of commonly used engineering materials [4], the values of Y_e is set to be in the range of $0.01\ GPa \leq Y_e \leq 400\ GPa$.

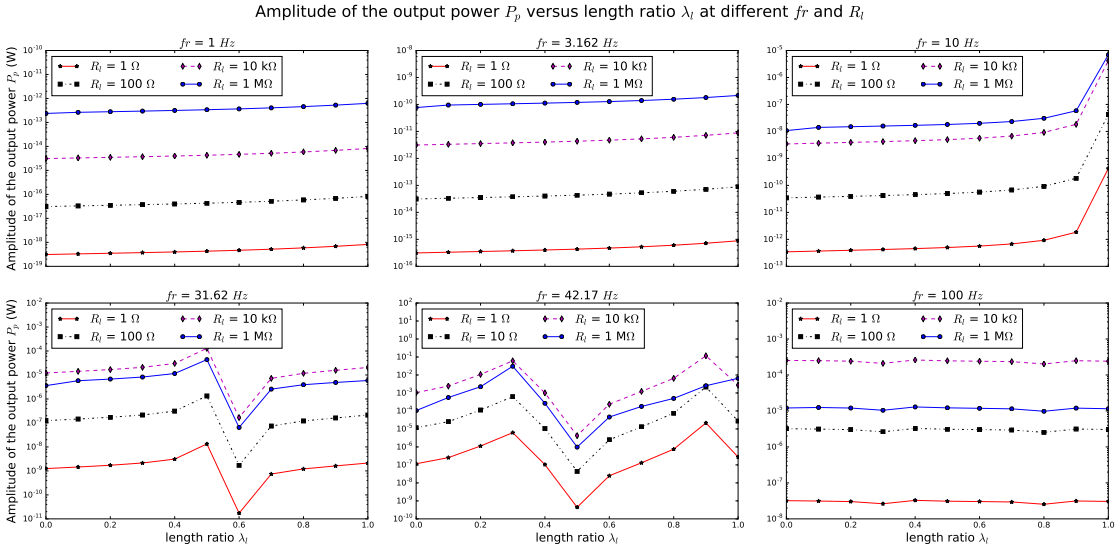

Figure 7: Output voltage V_p (amplitude) and output power P_p (amplitude) of the piezoelectric energy harvester with flexible extension versus length ratio λ_l at different frequency f and load resistance R_l. to be revised in the legend, add label (a), (b)

For each value of bending stiffness ratio λ_B, the base excitation problem is solved with respect to different base excitation frequency fr and load resistance R_l. In this process, the length ratio is fixed to be $\lambda_l = 0.3$ while its volumetric density is set to be $\rho_e = 1.38 \times 10^3\ kg/m^3$.

Firstly, the influence of base excitation frequency fr upon performance of the piezoelectric energy harvester is shown Figure 8 and Figure 9 at different values of load resistance R_l and bending stiffness ratio λ_B. To have a clear clue about the value of λ_B, it is found that for a Young's modulus of $Y_e = 0.01\ GPa$, the corresponding value of bending stiffness ratio is $\lambda_B = 2.39 \times 10^{-5}$, while for a Young's modulus of $Y_e = 200\ GPa$, the corresponding value of bending stiffness ratio is $\lambda_B = 0.478$.

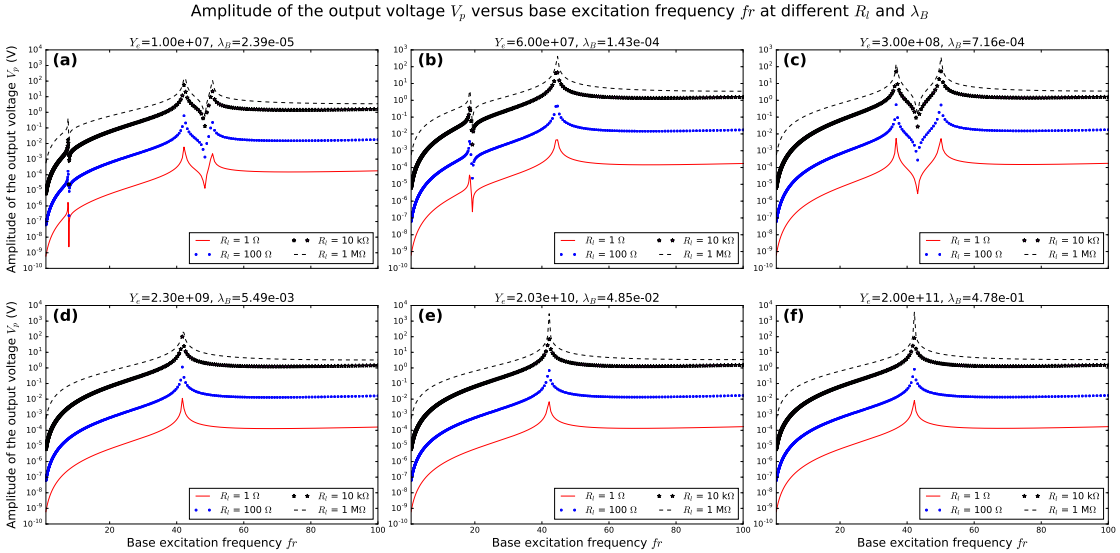

Figure 8: Output voltage V_p (amplitude) of the piezoelectric energy harvester with flexible extension versus base excitation frequency fr at different bending stiffness ratio λ_B and load resistance R_l. to be revised in the legend. change figure title

It is easily seen from Figure 8 and Figure 9 that, at the given values of λ_l and λ_m, bending stiffness ratio λ_B also affects frequency response of the proposed piezoelectric energy harvester with flexible extension, but in a different manner from length ratio λ_l.

When the bending stiffness ratio λ_B is very small, say $Y_e = 0.01\ GPa$, as shown in Figure 8(a)

and Figure 9(a), there exist multiple resonant modes in the considered frequency range. And some of the resonant modes are potential to be used for energy harvesting. With the increase of bending stiffness ratio λ_B, fewer resonant modes are present in the considered frequency range. For example, when $Y_e = 0.3\ GPa$, two resonant modes are present and when $Y_e = 2.3\ GPa$, only one resonant mode is present. As a result, less frequencies can be utilized for energy harvesting. That is to say, to achieve an energy harvesting capacity of wider frequency range, smaller bending stiffness ratio λ_B is preferred. Actually, from Figure 8 we can conclude that, a bending stiffness ratio λ_B in the order of 10^{-4} or lower is beneficial to the energy harvesting performance of the piezoelectric energy harvester with flexible extension. However, only changing the value of λ_B is not the best way to tune the energy harvesting performance of the piezoelectric energy harvester with flexible extension. It is seen from the previous subsection and this subsection that, the combination change of larger λ_l and lower λ_B serve better for this goal.

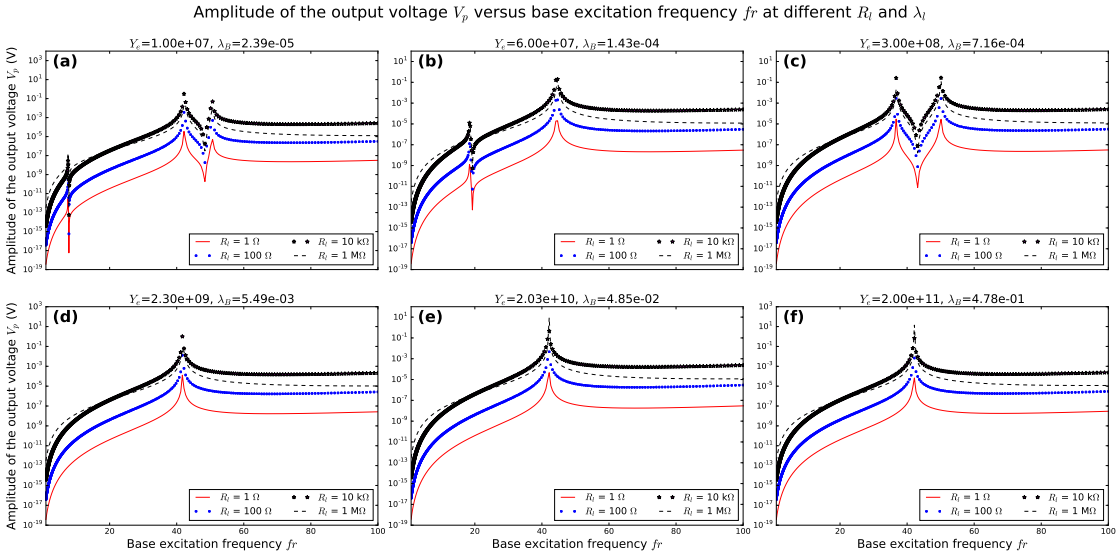

Figure 9: Output power P_p (amplitude) of the piezoelectric energy harvester with flexible extension versus base excitation frequency fr at different bending stiffness ratio λ_B and load resistance R_l. to be revised in the legend. change figure title

Similarly, for a set of chosen values of Y_e and therefore λ_B, we plot the amplitudes of output voltage V_p and output power P_p with respect to load resistance R_l at different base excitation frequencies fr in Figure 10 and Figure 11, respectively. It is easily seen that the amplitude of output voltage V_p increases in terms of increasing R_l and ultimately reaches a limit, which is actually the open-circuit output voltage. The amplitude of output power P_p will reaches its maximum at a critical value of R_l, which is dependent on the values of λ_B and fr.

The influence of bending stiffness ratio λ_B is shown by plotting the amplitudes of output voltage V_p and output power P_p relative to λ_B at different values of load resistance R_l and base excitation frequency fr, as shown in Figure 12 and Figure 13, respectively. It is found that for a low frequency base excitation, as shown in Figure 12(a) and (b), no big difference is seen when we change the values of λ_B. The amplitudes of output voltage V_p and output power P_p remain at a low level and the proposed piezoelectric energy harvester with flexible extension can not be used for energy harvesting. For a higher base excitation frequency fr, as shown in Figure 12(c) and (d) and Figure 13(c) and (d), a peak of V_p and P_p is found for certain value of λ_B. The output performance of the piezoelectric energy harvester with flexible extension is increased by changing the value of λ_B. For a further higher value of fr, as shown in Figure 12(e), the value of λ_B significantly change the amplitudes of output voltage V_p and output power P_p. To achieve higher energy harvesting performance, higher (in the order of 10^{-1}) or lower (in the order of 10^{-5}) values of λ_B are preferred against a moderate (in the order of 10^{-3}) value of λ_B. For the value of base excitation frequency $fr = 100\ Hz$, as shown in Figure 12(f), the value of λ_B is found again playing a minor role in changing the values of V_p and P_p.

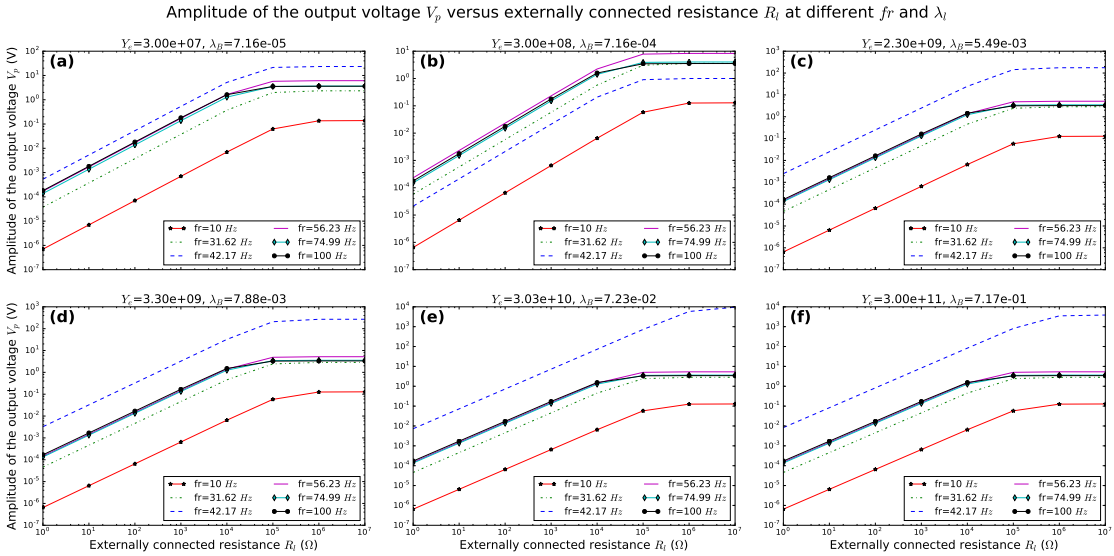

Figure 10: Output voltage V_p (amplitude) of the piezoelectric energy harvester with flexible extension versus bending stiffness ratio λ_B at different frequency fr and load resistance R_l. to be revised in the legend. change figure title

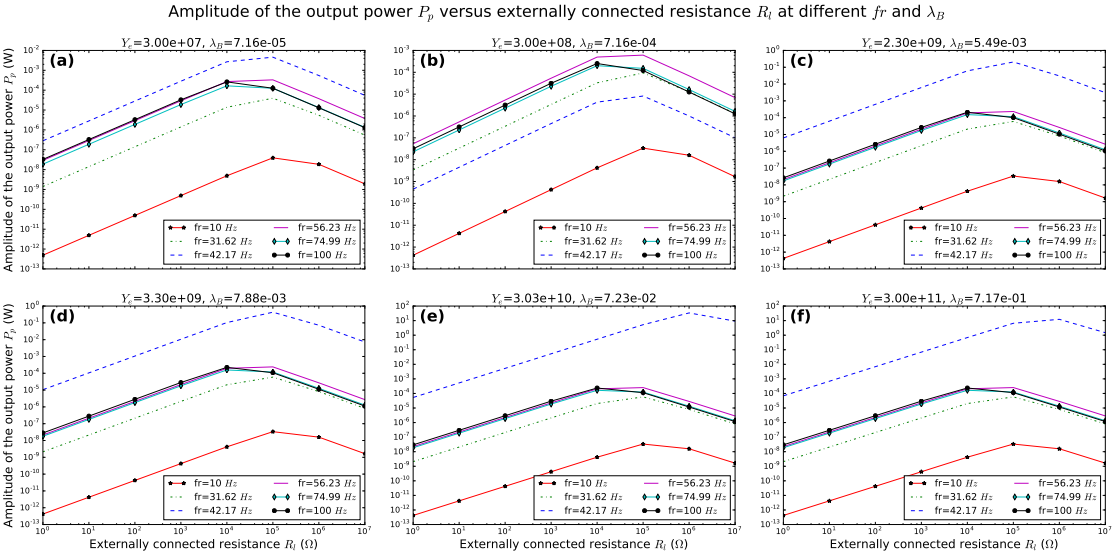

Figure 11: Output power P_p (amplitude) of the piezoelectric energy harvester with flexible extension versus bending stiffness ratio λ_B at different frequency fr and load resistance R_l. to be revised in the legend. change figure title

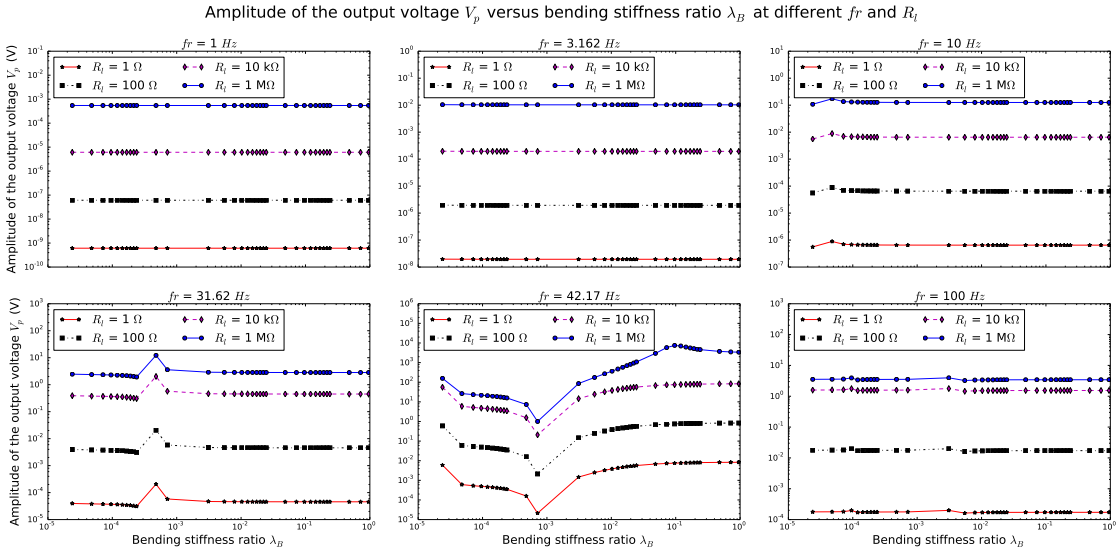

Figure 12: Output voltage V_p (amplitude) of the piezoelectric energy harvester with flexible extension versus bending stiffness ratio λ_B at different frequency fr and load resistance R_l.

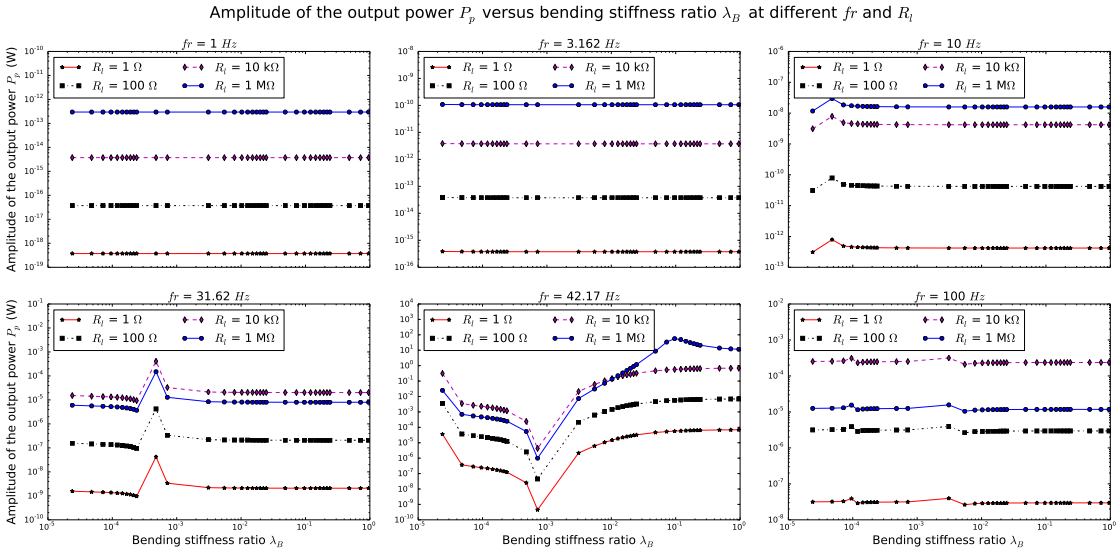

Figure 13: Output power P_p (amplitude) of the piezoelectric energy harvester with flexible extension versus bending stiffness ratio λ_B at different frequency fr and load resistance R_l.

3.3. Beam extension line density ρ_e or line density ratio λ_m

It is easily seen from the diagram that the change of extension length l_e have a great influence on the frequency response of the piezoelectric energy harvester. At the given values of λ_B and λ_m, the contained vibration modes in the frequency range considered does change with respect to the length ratio λ_l. When λ_l is relatively small, which is below 0.3 in our case, no extra vibration modes can be found in the frequency range of $1 - 100\ Hz$. Hence the energy harvesting performances of the proposed energy harvesters are similar to that of a pure cantilever beam piezoelectric energy harvester. (note: it will be better if I can compare the resonant energy harvesting performance in this case) With further increase of the length ratio λ_l, there begins to exist an extra resonant and anti-resonant mode in the considered frequency range. In this view, the change of length ratio actually expands the bandwidth of the energy harvesting performances. Even when the length ratio $\lambda_l = 1.0$, three resonant modes are found in the frequency range. The point to be noticed is the existence of anti-resonant mode, which largely narrows the bandwidth of the energy harvester. This accompanying characteristic is to be further investigated in the following research.

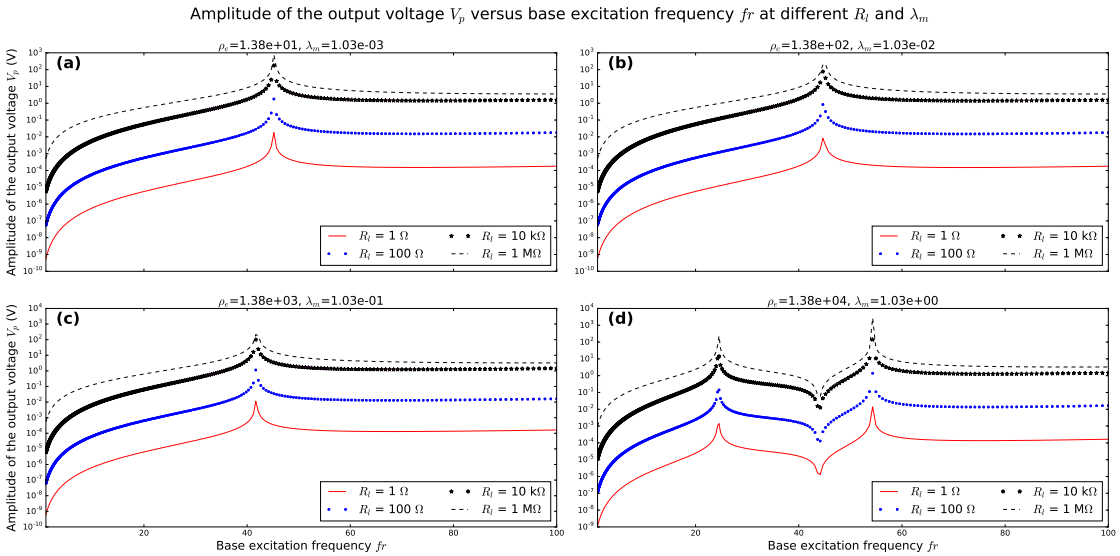

Figure 14: Output voltage V_p (amplitude) of the piezoelectric energy harvester with flexible extension versus base excitation frequency fr at different line density ratio λ_m and load resistance R_l.

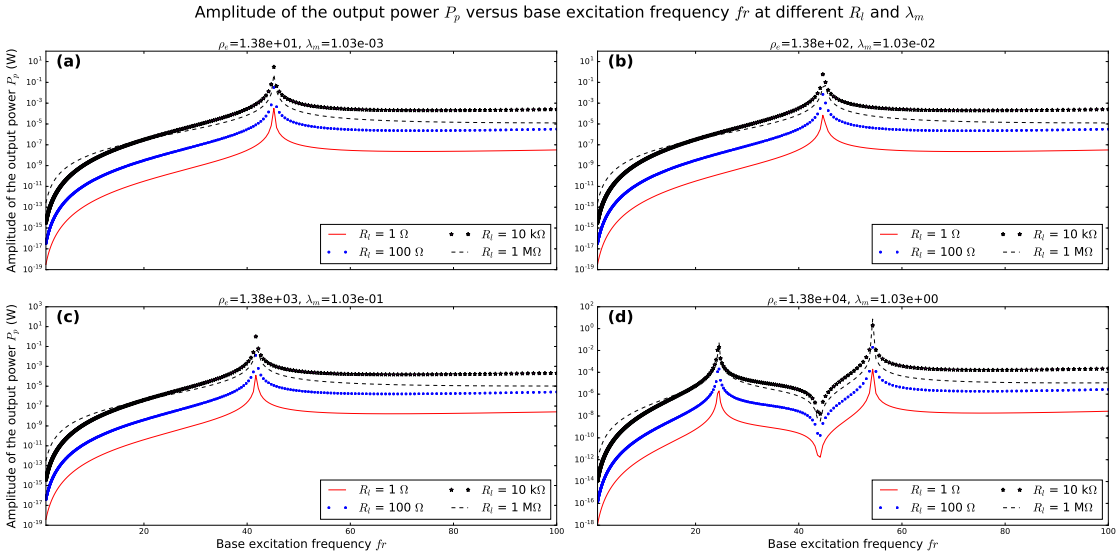

Figure 15: Output power P_p (amplitude) of the piezoelectric energy harvester with flexible extension versus base excitation frequency fr at different line density ratio λ_m and load resistance R_l.

It is easily seen from the diagram that the change of extension length l_e have a great influence on the frequency response of the piezoelectric energy harvester. At the given values of λ_B and λ_m, the contained vibration modes in the frequency range considered does change with respect to the length ratio λ_l. When λ_l is relatively small, which is below 0.3 in our case, no extra vibration modes can be found in the frequency range of $1 - 100\ Hz$. Hence the energy harvesting performances of the proposed energy harvesters are similar to that of a pure cantilever beam piezoelectric energy harvester. (note: it will be better if I can compare the resonant energy harvesting performance in this case) With further increase of the length ratio λ_l, there begins to exist an extra resonant and anti-resonant mode in the considered frequency range. In this view, the change of length ratio actually expands the bandwidth of the energy harvesting performances. Even when the length ratio $\lambda_l = 1.0$, three resonant modes are found in the frequency range. The point to be noticed is the existence of anti-resonant mode, which largely narrows the bandwidth of the energy harvester. This accompanying characteristic is to be further investigated in the following research.

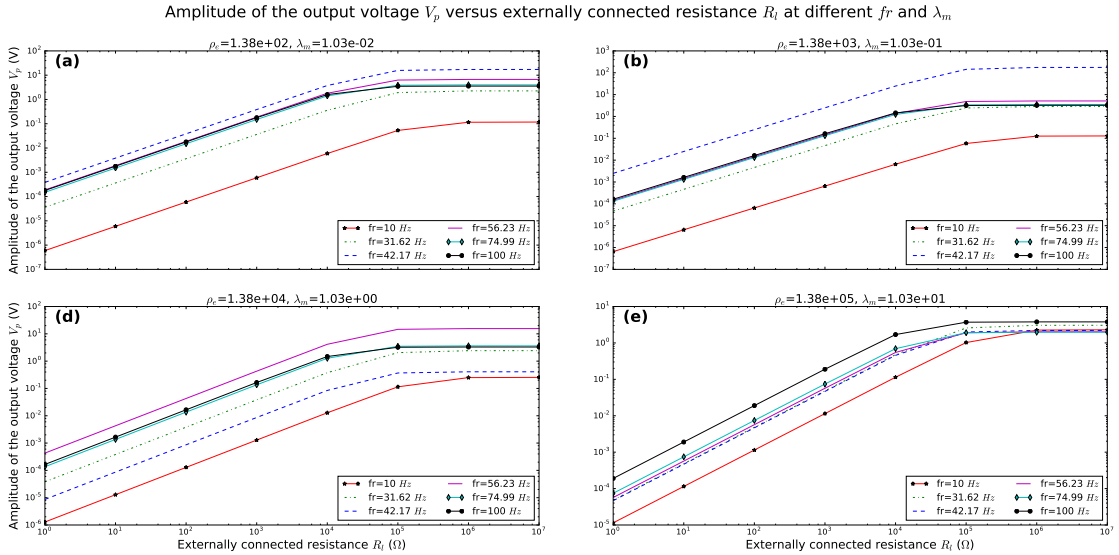

Figure 16: Output voltage V_p (amplitude) of the piezoelectric energy harvester with flexible extension versus line density ratio λ_m at different frequency fr and load resistance R_l.

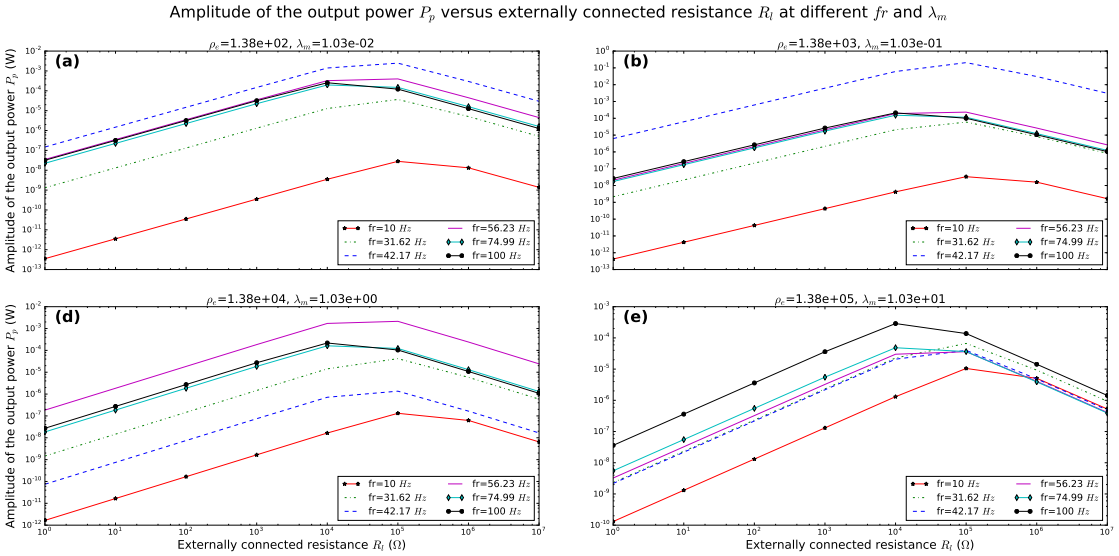

Figure 17: Output power P_p (amplitude) of the piezoelectric energy harvester with flexible extension versus line density ratio λ_m at different frequency fr and load resistance R_l.

It is easily seen from the diagram that the change of extension length l_e have a great influence on the frequency response of the piezoelectric energy harvester. At the given values of λ_B and λ_m,

the contained vibration modes in the frequency range considered does change with respect to the length ratio λ_l. When λ_l is relatively small, which is below 0.3 in our case, no extra vibration modes can be found in the frequency range of $1 - 100\ Hz$. Hence the energy harvesting performances of the proposed energy harvesters are similar to that of a pure cantilever beam piezoelectric energy harvester. (note: it will be better if I can compare the resonant energy harvesting performance in this case) With further increase of the length ratio λ_l, there begins to exist an extra resonant and anti-resonant mode in the considered frequency range. In this view, the change of length ratio actually expands the bandwidth of the energy harvesting performances. Even when the length ratio $\lambda_l = 1.0$, three resonant modes are found in the frequency range. The point to be noticed is the existence of anti-resonant mode, which largely narrows the bandwidth of the energy harvester. This accompanying characteristic is to be further investigated in the following research.

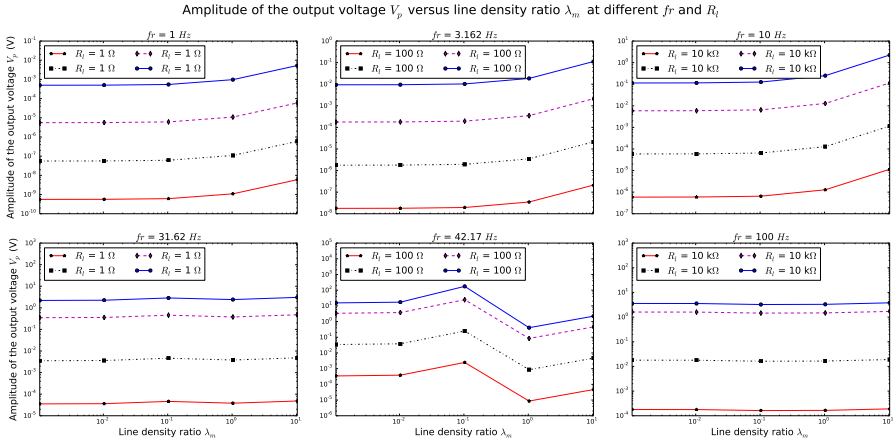

Figure 18: Output voltage V_p (amplitude) of the piezoelectric energy harvester with flexible extension versus line density ratio λ_m at different frequency fr and load resistance R_l.

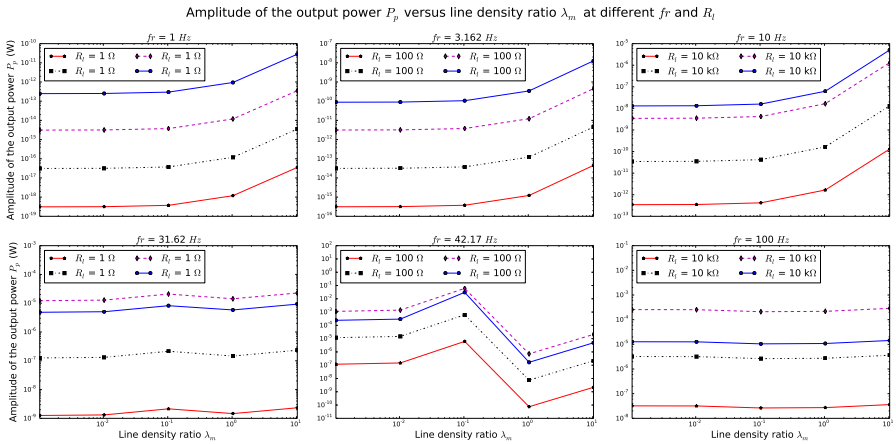

Figure 19: Output power P_p (amplitude) of the piezoelectric energy harvester with flexible extension versus line density ratio λ_m at different frequency fr and load resistance R_l.

It is easily seen from the diagram that the change of extension length l_e have a great influence on the frequency response of the piezoelectric energy harvester. At the given values of λ_B and λ_m, the contained vibration modes in the frequency range considered does change with respect to the length ratio λ_l. When λ_l is relatively small, which is below 0.3 in our case, no extra vibration modes can be found in the frequency range of $1 - 100\ Hz$. Hence the energy harvesting performances of the proposed energy harvesters are similar to that of a pure cantilever beam piezoelectric energy harvester. (note: it will be better if I can compare the resonant energy harvesting performance in this case) With further increase of the length ratio λ_l, there begins to exist an extra resonant and anti-resonant mode in the considered frequency range. In this view, the change of length ratio actually expands the bandwidth of the energy harvesting performances. Even when the length ratio $\lambda_l = 1.0$, three resonant modes are found in the frequency range. The point to be noticed is the

existence of anti-resonant mode, which largely narrows the bandwidth of the energy harvester. This accompanying characteristic is to be further investigated in the following research.

4. Discussion

5. Conclusion

Here in this contribution, we investigate the method of flexible extension to tune the energy harvesting performance of piezoelectric cantilever energy harvester.

Reference

[1] Erturk A, Inman DJ. An experimentally validated bimorph cantilever model for piezoelectric energy harvesting from base excitations. Smart materials and structures. 2009;18(2):025009.

[2] Park CH. Dynamics modelling of beams with shunted piezoelectric elements. Journal of Sound and vibration. 2003;268(1):115–129.

[3] Driscoll TA, Hale N, Trefethen LN. Chebfun guide. Pafnuty Publications, Oxford; 2014.

[4] Warlimont H, Martienssen W. Springer Handbook of Materials Data. Springer; 2018.